



UNIVERSITY COLLEGE LONDON

MPHYM000: RESEARCH PROJECT IN MEDICAL PHYSICS

Rapid Prototyping Of Ultrasound Transducers

Samuel J Searles-Bryant

Supervisors: Dr Bradley TREEBY,
Dr Ben Cox, Dr Elly MARTIN

April 3, 2017

I, Samuel J Searles-Bryant, confirm that the work presented in this report is my own. Where information has been derived from other sources, I confirm that this has been indicated in the work.

Abstract

Arrays of ultrasound transducers for therapeutic applications (*e.g.* High Intensity Focused Ultrasound) can have large costs and lead times. Rapid prototyping technologies, particularly 3D printing, can be used to manufacture many devices quickly and at a low cost. This project demonstrates the use of 3D printing to build single-element ultrasound transducers, which can be used to generate arbitrary acoustic fields.

An iterative design process was used to develop simple transducer designs and build two large (38 mm diameter) transducers, costing approximately £30 each. These were characterised acoustically and the temperature response was studied. The design was developed to build two smaller (10 mm diameter) transducers, costing approximately £26 and suitable for use in arrays.

The use of focusing lenses and acoustic kinoforms to influence the shape of the acoustic field was demonstrated. These were designed to attach to the 3D printed transducers so that multiple field geometries could be generated using a single transducer quickly and for a very low cost. These attachments cost only £2.50 to build.

This project has demonstrated that 3D printed ultrasound transducers can generate designed acoustic fields for a fraction of the cost of commercially available transducers. Designs and processes for effectively manufacturing single-element transducers have been established and are well-placed to be developed to allow the construction of multi-element arrays in the future.

Acknowledgements

I would like to thank my supervisors—Dr Bradley Treeby and Dr Ben Cox—for devising this project and providing guidance throughout the year.

I would especially like to thank Dr Elly Martin for her mentorship during the practical elements of this project. I am particularly grateful for her support with the experiments to measure the field generated by my transducers and for generously providing a library of MATLAB functions with which to process the data collected.

Advice given by Louis Robertson regarding 3D printing materials and techniques and his insights into applications of multi-element arrays of ultrasound transducers in neuromodulation were greatly appreciated.

Michael Brown provided functions and advice used to design and model the kinoform lens. Srinath Rajagopal performed impedance measurements on my behalf. I am grateful to the rest of the Biomedical Ultrasound Group at UCL for their advice and criticism throughout the project.

I am particularly grateful for the assistance given by Eve Hatton with 3D printing. I would also like to thank Marco Endrizzi, who generously performed x-ray imaging of a transducer on my behalf.

Dr Xiao Liu provided assistance with impedance measurements. Andrew Maxwell from the University of Washington shared with us several 3D printing designs and a script to calculate values for the impedance matching network. The Bartlett Manufacturing and Design Exchange at the Bartlett School of Architecture assisted with some 3D printing where facilities were not available in Medical Physics & Biomedical Engineering.

My thanks are extended to the staff of Ferroperm Piezoelectrics for providing samples of PZT, with which I built the transducers. I would also like to acknowledge the generosity of the staff of Tungsten Alloys for making arrangements to supply us with tungsten powder in unusually small quantities.

Contents

1	Introduction	1
1.1	Background and Motivation	1
1.2	Rapid Prototyping	1
1.3	Aims and Objectives	2
2	Ultrasound Transducers	3
2.1	Piezoelectric Elements	3
2.2	Quarter Wave Matching Layer	4
2.3	Electrical Impedance Matching	5
2.4	Backing Material	7
2.5	Lenses	7
3	Large Transducer Elements	9
3.1	Transducer 1	9
3.1.1	Design	9
3.1.2	Manufacture	12
3.1.3	Acoustic Characterisation	13
3.2	Development of Design (Transducer 2)	18
3.2.1	Modifications and Improvements to Design	19
3.2.2	Acoustic Characterisation	21
3.2.3	Temperature Response	24
3.3	Conclusions	25
4	Smaller Transducer Elements	29
4.1	Design	29
4.2	Design Development	30
4.3	Manufacture	31
4.4	Conclusions	34

5 Detachable Lenses	35
5.1 Focusing Lens	35
5.1.1 Design	35
5.1.2 Acoustic Characterisation	35
5.2 Acoustic Kinoform	38
5.3 Conclusions	39
6 Summary & Conclusions	41
6.1 Summary	41
6.2 Future Development	42
Appendices	43
A List of Designed Parts	43
References	47

Chapter 1

Introduction

1.1 Background and Motivation

High Intensity Focused Ultrasound (HIFU) (also known as Focused Ultrasound Surgery (FUS)), involves focusing an ultrasound beam to cause intense heating, which kills tissue in the focal area. HIFU transducers are often driven at frequencies of 0.5–10 MHz.^[1] Focused ultrasound can also be used for neuromodulation.^[2] Many of these applications require large arrays of transducer elements, which can be particularly costly and time-consuming to build: a 32-element array can cost up to \$50 000 and take up to a year to fabricate (this equates to a per-element cost of approximately \$1500).^[3]

To overcome these limitations, the Biomedical Ultrasound Group (BUG) at University College London (UCL) plan to develop a system to use Rapid Prototyping (RP) techniques to manufacture transducer arrays quickly and at low cost. This project is the first stage in that process, demonstrating the design of single-element transducers and establishing a workflow for building transducers and acoustic lenses.

1.2 Rapid Prototyping

In this project “RP techniques” refers, specifically, to 3D printing. 3D printing of ultrasound transducers has been demonstrated successfully in the past:^{[3],[4]} Kim *et al.*^[3] produced a 32-element array for approximately \$5000 (approximately \$150 per element) by printing the transducer housings and the array frame. These transducers provided a “solid acoustic performance”

1.3 Aims and Objectives

at a low cost.

It has also been demonstrated that piezoelectric elements can be manufactured using additive manufacturing methods.^{[5]-[7]} These methods use a piezoelectric-composite slurry to form custom piezoelectric elements.

The specific 3D printing technology used for this project was stereolithography (SLA), using an Objet30 printer (Stratasys). SLA was chosen over fused deposition modeling (FDM) (another popular 3D printing technology) because FDM can introduce pockets of air into the printed object, which would make it unsuitable for transmitting ultrasound.

1.3 Aims and Objectives

This project aims to demonstrate that ultrasound transducers can be built quickly and at low cost using RP techniques. In order to overcome the high cost and lead times associated with manufacturing ultrasound arrays, BUG would like to be able to design a catalogue of 3D printable parts to be used to test array designs.

The specific objectives of this project were

1. Design several iterations of rapidly prototyped ultrasound transducers using an iterative design process;
2. Characterise the acoustic and thermal response of the transducers;
3. Investigate the use of detachable lenses to create specific ultrasound fields.

Chapter 2

Ultrasound Transducers

Ultrasound transducers have six main component parts: a piezoelectric element, a quarter-wave matching layer (QWML), a driving circuit, backing material, a lens, and the enclosure (the transducer housing) (Fig. 2.1).

2.1 Piezoelectric Elements

A piezoelectric material is a material which generates an electric field when it is compressed and is compressed when an electric field is applied across it.^[8] When an oscillating field is applied across a piezoelectric element it will oscillate mechanically, producing a pressure wave.

The piezoelectric elements used for this project were lead zirconate titanate (PZT) discs, the faces of which were covered by silver electrodes. The first iterations of the single-element transducer were built using large PZT discs with a diameter of 38 mm and a thickness of 2 mm. The smaller transducers were built using smaller discs with a diameter of 10 mm and a thickness of 2 mm. The discs were provided as samples by Ferroperm Piezoceramics; they are made from Pz26 (also called Navy I), a variant of PZT which is particularly well suited to medical therapeutic transducers due to its hardness and high mechanical quality factor.^[9]

An air-backed transducer has a central frequency

$$f_0 = \frac{c}{2L}, \quad (2.1)$$

where L is the thickness of the piezoelectric element, and c is the speed of sound inside the element.^[10] The speed of sound inside the element is double

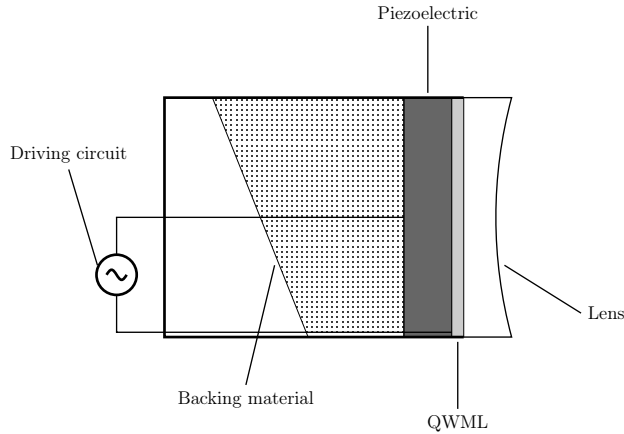


Figure 2.1: A schematic of a cross-section of a typical single element–ultrasound transducer. The significant components are labelled; these are contained within the transducer housing.

the frequency constant; the frequency constant of the thickness oscillation of a thin disk of Pz26 polarised in the thickness direction is 2040 Hz m, therefore $f_0 = 1.02$ MHz; this is suitable for High Intensity Focused Ultrasound (HIFU) therapies.^[11] The transducers built for this project were therefore designed to be driven at a frequency of 1 MHz.

The acoustic impedance of the PZT disc is

$$Z = \rho c, \quad (2.2)$$

where ρ is the density of the disc.^[10] The density of Pz26 is 7.70 g cm^{-3} , therefore the impedance is 31.416 MRayl.

2.2 Quarter Wave Matching Layer

In order to minimise the reflection at the boundary between the front of the transducer and the medium into which ultrasound is propagating, an acoustic matching layer, which has a thickness of 1/4 of a wavelength, is inserted in front of the piezoelectric element. This layer has two functions: to match the acoustic impedance of the piezoelectric element to that of the medium, and to maximise the transmission of acoustic energy by interference effects. The QWML matches the acoustic impedance of the PZT disc to the transducer housing best when its impedance is the geometric mean of these

values. The QWML's thickness causes the resultant reflected and transmitted waves interfere in the medium and in the transducer to reinforce transmitted waves and to cancel reflected waves. Thus the QWML acts to maximise the amplitude of the transmitted ultrasound wave.

The QWML used for these transducers was created using a recipe from Kim *et al.*^[3]: a mix of 13% epoxy resin and 87% tungsten powder by weight. The epoxy resin used was a standard two-part epoxy adhesive (Araldite, ARA-400001): a two-part mixture. The tungsten powder was a pure tungsten powder with 5 µm particles (Tungsten Alloys).

Webster^[12] lists the speed of sound in a tungsten and epoxy resin mixture as $(2551 \pm 130) \text{ m s}^{-1}$. Therefore the thickness of the QWML should be 0.63 mm. However, the resolution of the Objet30 printer is only 100 µm. Although the Computer Aided Design (CAD) models were designed with a QWML thickness of 0.63 mm, this precision could not be guaranteed in the printed parts.

Since the acoustic impedance of the PZT disc is 31.416 MRayl (Section 2.1) and the impedance of VeroBlackPlus (the material used to print the transducer housings, see Section 3.1.1) is 2.9 MRayl, the QWML should have an impedance of approximately 9.5 MRayl. However, since the impedance of the epoxy-tungsten mix is unknown, this cannot be verified. The recipe from Kim *et al.*^[3] is taken at face value: it is evident from measuring the output of the transducers that have been built that this mixture is adequate, even if not perfect (Sections 3.1.3 and 3.2.2). A full analysis of the acoustic impedance of QWML composites is beyond the scope of this project.

2.3 Electrical Impedance Matching

To maximise the transfer of power from the driving circuit to the transducer, the signal is applied through an electrical impedance matching network. The networks used for the transducers in this project were simple inductor-capacitor pairs (Fig. 2.2). The values of these components can be determined using the quadratic formula to determine the desired impedance of the matching network, X_n . If the real component of the transducer's impedance ($Z_t = R_t + jX_t$) is smaller than the real component of the source impedance

2.3 Electrical Impedance Matching

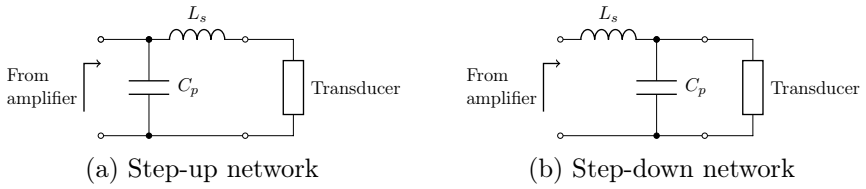


Figure 2.2: Impedance matching networks comprising a capacitor and an inductor. These circuits (a) increase and (b) decrease the apparent impedance of the transducer to maximise the transfer of power.

$(Z_s = R_s + jX_s)$, a step-up network is used (Fig. 2.2a). In this case,

$$X_n^2 - \frac{2R_t X_s}{R_s - R_t} X_n - \frac{R_t(R_s^2 + X_s^2)}{R_s - R_t} = 0 \quad (2.3)$$

If the real component of the transducer's impedance is larger than the real component of the source impedance, a step-down network is used (Fig. 2.2b). In this case,

$$X_n^2 - \frac{2R_s X_t}{R_s - R_t} X_n + \frac{R_s(R_t^2 + X_t^2)}{R_s - R_t} = 0 \quad (2.4)$$

The capacitance of the capacitor in both networks is

$$C_p = \frac{1}{X_n \omega}, \quad (2.5)$$

where ω is the angular frequency of the signal (*i.e.* $\omega = 2\pi f = 6.28 \times 10^6$ for $f = 1$ MHz). For the step-up network, the inductance is

$$L_s = \frac{X_n(R_s - R_t) - R_s X_t - R_t X_s}{R_s \omega}. \quad (2.6)$$

For the step-down network, the inductance is

$$L_s = \frac{X_s - \Im\left(\frac{Z_c Z_t}{Z_c + Z_t}\right)}{\omega}. \quad (2.7)$$

where $Z_c = \frac{1}{j\omega C_p}$ is the impedance of the capacitor. These equations, the circuit designs, and a MATLAB script to calculate the component values were provided by Adam Maxwell of the University of Washington.^[13]

2.4 Backing Material

Diagnostic ultrasound transducers often contain a backing material to prevent the piezoelectric element from ringing, shortening the emitted pulse and increasing the bandwidth. However, ultrasound transducers for therapeutic applications often contain no backing material; instead they are air-backed. Air-backed transducers transmit a higher amplitude pressure wave into the medium, with a lower bandwidth (*i.e.* a high quality factor). This is desired for therapeutic applications.

Although the transducers built for this project are intended to be air-backed, the housings of the large transducers were filled with a two-part soft urethane foam (Polycraft, 010) to ensure that they would be water-proof and to hold the matching network and a thermocouple in position (see Chapter 3). This foam has a low density (approximately 0.125 g cm^{-3})^[14] and after setting consists mostly of air bubbles.

2.5 Lenses

Lenses can be used to create specific acoustic fields with a transducer. Focusing lenses can direct energy to a specific single focal region. Acoustic kinoforms use phase profiling to generate arbitrary acoustic fields using holograms; the shape of the acoustic field is limited only by the diffraction limit.^[15] These holograms create a varying phase profile across the surface of a lens; the interference from this phase profile creates the desired acoustic field.

Spherical bowl lenses, for focusing the acoustic pressure at a single point, are commonly used in HIFU treatments to direct energy to a specific location. The focal length of a spherical lens is

$$f = \frac{R_1 R_2}{(1 - c_1/c_2)[d(c_2/c_1 - 1) - R_1 + R_2]}, \quad (2.8)$$

where R_1 and R_2 are the radii of curvature of each side, c_1 is the speed of sound in the lens, c_2 is the speed of sound in the surrounding medium, and d

is the thickness of the lens.^[16] If one side of the lens is flat this becomes

$$\begin{aligned} f &= \frac{-R}{c_1/c_2 - 1} \\ &= \frac{-R}{n_a - 1} \\ \Rightarrow R &= -f \left(\frac{c_1}{c_2} - 1 \right). \end{aligned} \tag{2.9}$$

Chapter 3

Large Transducer Elements

The first iteration of the design was a proof-of-concept, which was built with the aim of demonstrating that a functioning transducer could be built at low cost using Rapid Prototyping (RP) techniques. The second iteration was built to improve on the shortcomings of the first design: the lessons learned from the manufacture and testing of Transducer 1 were taken into account to design a transducer with an improved acoustic performance.

Each of the transducers that was built was characterised in an acoustic scanning tank (Sections 3.1.3 and 3.2.2) and compared to simulations of comparable “ideal” transducers to confirm that the field generated was similar to that which would be expected.

3.1 Transducer 1

3.1.1 Design

The first transducer design had 2 parts: the transducer housing—including a focusing lens—and a cap. This simple design was modelled on the transducers previously built by Kim *et al.*^[3].

Transducer Housing

The first design for the transducer housing was a hollow cylinder, open at one end with a spherical bowl at the other (Fig. 3.1). The cylinder was 5 cm long and its outer diameter was 43 mm. A ridge the thickness of the quarter-wave matching layer (QWML) ran around the edge of the inside base of the cylinder. This held the lead zirconate titanate (PZT) disc away from

3.1 Transducer 1

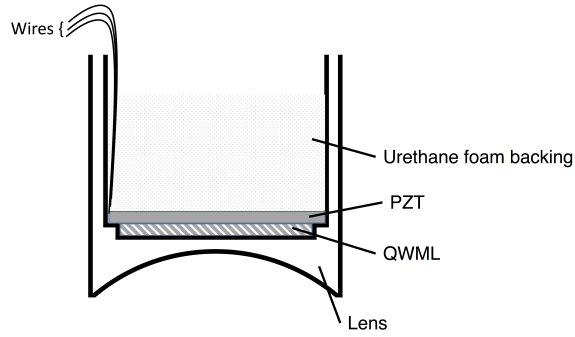


Figure 3.1: Diagram of the design of the housing for Transducer 1. This diagram also illustrates the placement of the PZT disc and the QWML inside the housing. It does not contain the electronic circuits.

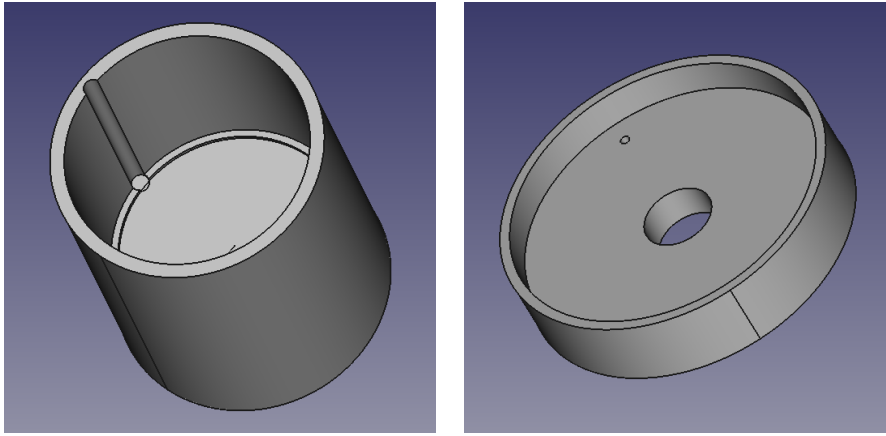
the base of the housing and created a gap for the QWML. A channel on the inside face of the cylinder allowed a wire to connect to the underside of the PZT. These features can be seen in Fig. 3.2a.

Transducer 1 was printed with the VeroBlackPlus (Stratasys, RGD875) material. VeroBlackPlus was chosen because it is a low cost material with acoustic properties that are suitable for ultrasound devices. The material has been investigated by Nikitichev *et al.*^[17] such that its acoustic properties are known; these include the sound speed ($(2495 \pm 8) \text{ m s}^{-1}$), acoustic impedance (2.9 MRayl), and acoustic attenuation ($(3.1 \pm 0.1) \text{ dB cm}^{-1} \text{ Hz}^{-1}$).

The first model for the housing had an internal diameter of 38 mm; this did not allow the PZT disc to be inserted. The design was modified to allow a 0.25 mm gap around the disc (*i.e.* the internal diameter was 38.5 mm), which allowed the disc to move easily into position.

The transducer cap allows the electronics to be placed inside a waterproof housing. The cap fits over the open end of the transducer housing and has two holes: one for the BNC socket, which connects the transducer to the driving circuit, and one for the thermocouple.

The first iteration of the design for the cap was too thick (5 mm): the BNC socket's screw thread was not long enough for the nut to make a firm connection. A second iteration of the design reduced the thickness of the top part of the cap to 4 mm.



(a) Notable features in the housing are the ridge on which the PZT disc sits and the channel for the wire that connects to the front face of the disc.
 (b) The cap has a central hole for a BNC socket and a smaller hole for a thermocouple cable.

Figure 3.2: Computer Aided Design (CAD) models of (a) the housing and (b) the cap used in Transducer 1.

Lens

A lens was built into the housing of Transducer 1. The lens was a $f/1$ lens, meaning the focal length was equal to the width of the element (*i.e.* 38 mm). The curvature of this lens was calculated according to standard formulae (Section 2.5 and Eq. (2.9)) to be 23.5 mm.

The thinnest part of the lens on Transducer 1 was 0.1 mm thick. This distance was chosen to minimise the attenuation of the ultrasound signal as it travelled through the housing. However, a hole formed at this point when the part was printed (see Section 3.1.2).

Electronics

Transducer 1 has a BNC socket in the cap. The impedance matching circuit was placed inside the transducer housing and embedded in the urethane foam backing material.

Transducer 1 also included a k-type thermocouple (RS Pro, 363-0250) in order to characterise the thermal response of the transducer. This was inserted through a hole in the transducer cap and the junction sat above the rear electrode of the PZT disc.

3.1 Transducer 1

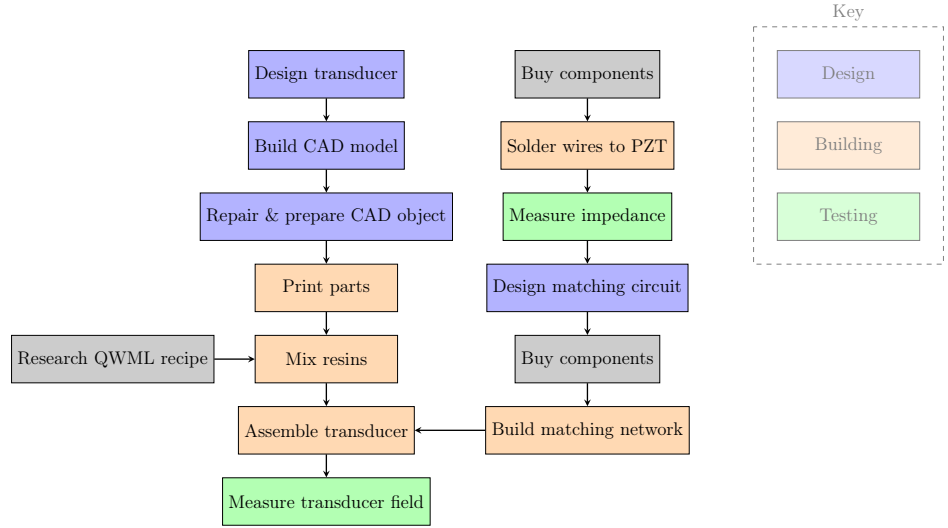


Figure 3.3: Flowchart describing the manufacturing process for Transducer 1. The process has multiple concurrent strands, which culminate in the assembly of each individual section before the transducer can be tested.

3.1.2 Manufacture

The process of assembling a working transducer had several concurrent workflows (Fig. 3.3). Once the transducer housing had been designed, a 3D model was made in 3D CAD software (FreeCAD, open source).^[18] This model was then prepared for printing using another software package (Autodesk meshmixer) and sent to be printed on the Objet30 (Stratasys) 3D printer.¹

Concurrently, some of the electrical components were purchased (including the BNC sockets and wires) and the wires were soldered to the electrodes on the face of the PZT disc. The PZT's electrical impedance was then measured.² The complex impedance of the PZT disc, immersed in water, at 1 MHz was $(0.767\ 123 + 2.360\ 353i)\ \Omega$. This was matched to the source impedance ($50\ \Omega$) with a step-up network (see Section 2.3 and Fig. 2.2a). The values of the components in the step-up network were calculated using a MATLAB script (see Section 2.3). The script calculated the ideal values of the components to be 5.1679 nF and $5.773\text{ }\mu\text{H}$. The matching network that was built comprised three capacitors in parallel ($2 \times 1.5\text{ nF}$ capacitors (KEMET,

¹The print was processed by Eve Hatton of the Dept Medical Physics & Biomedical Engineering.

²This measurement was conducted by Srinath Rajagopal at the National Physics Laboratory.

C921U152MUWDBA7317) and a 2.2 nF capacitor (Vishay, 440LD22-R)) equivalent to a single 5.2 nF capacitor, and a 5.6 μ H inductor (EPCOS, B78108S1562K000).

A recipe for the QWML was identified and the component parts were purchased (see Section 2.2). The urethane foam (Polycraft, 010) was purchased and tested to confirm the quantity needed to fill the transducer housing. It was determined that approximately 7 g was sufficient to cover the necessary components inside the housing. It was also confirmed that the foam would expand around components without moving them significantly: a preparation of the expanding foam was placed in a cup containing a selection of wire components and safety pins. As the foam expanded the components were not moved from their original positions and became embedded in the foam. A small cup was made from the foam and filled with water to verify its efficacy as a waterproofing layer.

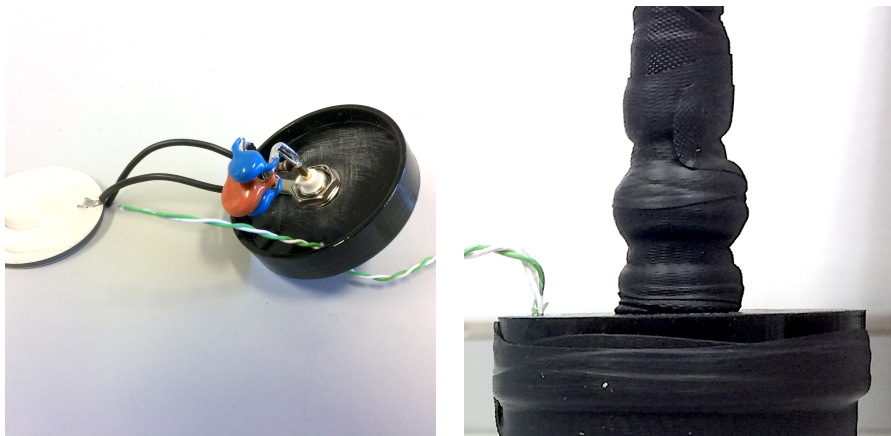
Transducer 1 was assembled in one session. The matching network was soldered to the BNC socket through the large hole in the cap and the thermocouple wire was threaded through the smaller hole Fig. 3.4a. The wires connected to the PZT disc were soldered to the matching network. A layer of tungsten loaded epoxy was pasted on the front face of the PZT disc and it was lowered into position in the housing. Approximately 7 g of the urethane foam mixture was poured into the cavity of the housing and the lid was placed on top. The edges around the thermocouple wire, the BNC connector, and the join between the transducer housing and its cap were sealed with a standard preparation of the epoxy adhesive (Araldite, ARA-400001).

Once sufficient time had been allowed for the epoxy adhesive mixtures to cure (approximately 24 hours), a coaxial cable was attached to the transducer and the socket was wrapped in self-amalgamating tape (RS Pro, 494-449) to keep water out (Figs. 3.4b and 3.5).

3.1.3 Acoustic Characterisation

The acoustic field generated by Transducer 1 was measured in an acoustic scanning tank. The collected data were analysed and compared to simulations of the expected response. The differences between the simulated and measured fields were investigated to inform the development of the design of the transducer.

3.1 Transducer 1



(a) The electrical impedance matching network, BNC socket, and thermocouple cable attached to the cap for Transducer 1.

(b) A coaxial cable is attached to the BNC socket on Transducer 1. The connection is wrapped in self-amalgamating tape to keep water out.

Figure 3.4: Two stages of the manufacture of Transducer 1.

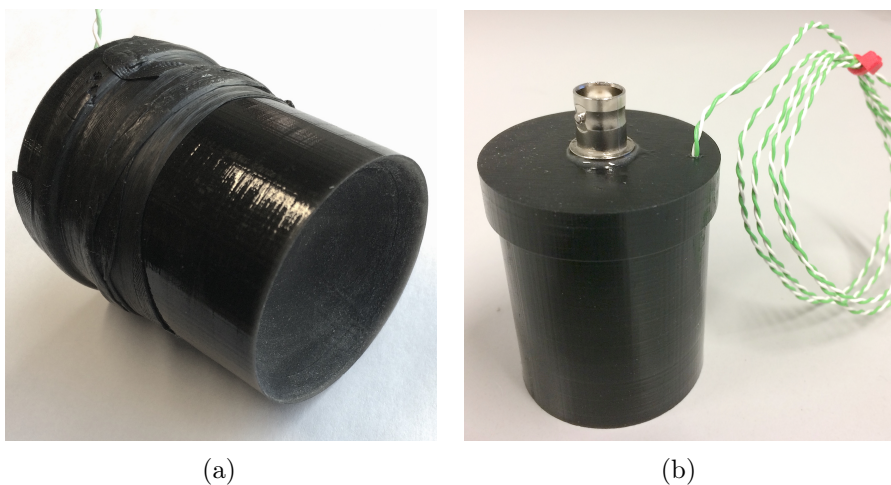


Figure 3.5: Transducer 1.

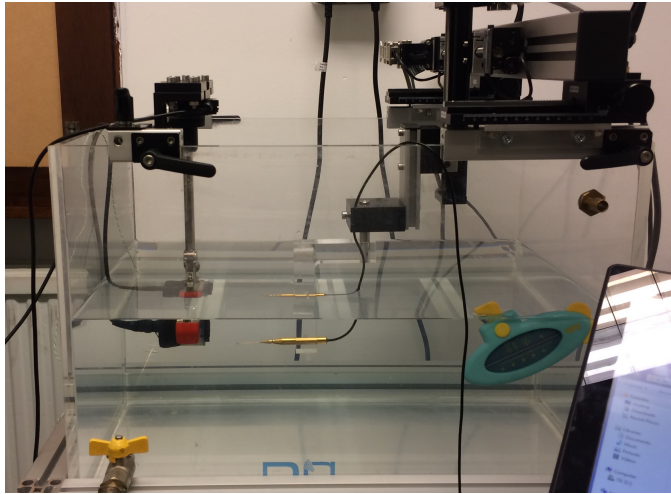


Figure 3.6: The experimental setup for the measurement of the acoustic field generated by a transducer. The transducer (left) is held in place while a needle hydrophone (centre) is moved in a plane perpendicular to the propagation of the field.

Scanning Tank Measurements

To measure the acoustic field generated by the transducer, it was immersed in a tank of deionised water (Fig. 3.6). The transducer was driven with a 10 V peak-to-peak sine wave from a signal generator (Agilent, 33522A). The signal was applied in 52-cycle bursts. The transducer was held in place while a 0.5 mm needle hydrophone (Precision Acoustics, 2290) was moved in a plane perpendicular to the propagation of the field (*i.e.* the XY-plane) by motorised axes (Velmex Inc, XN10-0060-M01-71). The transducer was aligned with the motorised axes by locating the position of the beam maximum in several planes and adjusting the orientation of the transducer by eye.

The pressure at the tip of the hydrophone was recorded during a 10 μ s period using a DC coupler (Precision Acoustics, DCPS450) plugged into an oscilloscope (Agilent, DSO-X 3024A) and the UMS Scanning Tank software (Precision Acoustics) at each point in a 75×75 point grid, with a grid spacing of 0.6 mm. The time window was chosen so that the recorded signal would be equivalent to the signal recorded if the transducer were transmitting in continuous-wave mode (*i.e.* signal had arrived from all parts of the transducer face). The recorded pressure data were saved to disk by the software.

3.1 Transducer 1

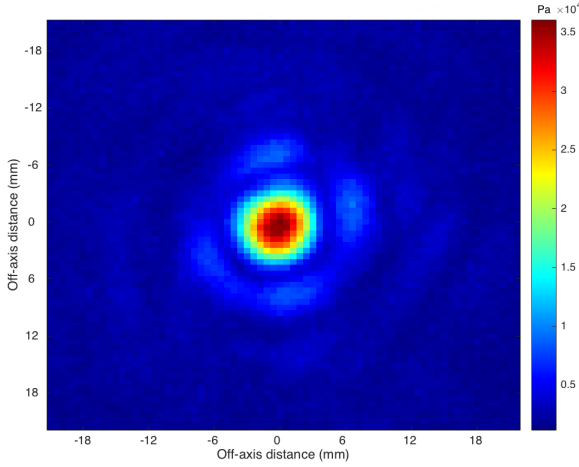


Figure 3.7: The pressure across a plane 45 mm from Transducer 1, driven at 10 V peak-to-peak.

Analysis of Acoustic Field Measurements

The recorded pressure data were processed in MATLAB (MathWorks, R2015b) using functions provided by Dr Elly Martin.^[19] The recorded plane (Fig. 3.7) was used to calculate the pressure amplitude at all points along the beam axis using the Rayleigh integral (Fig. 3.8). This shows that the transducer has a focus at approximately the expected distance (38 mm) from the transducer, however it is slightly closer.

An XZ-plane through the acoustic field was also calculated using the Rayleigh integral. This plane shows the shape of the acoustic field generated by Transducer 1 and can be compared to a simulation of an ideal bowl transducer with the same aperture size and focal length (Fig. 3.9). The comparison demonstrates that Transducer 1 has a much larger focal area than expected. In order to investigate this, the Rayleigh integral was used to calculate the pressure at the surface of the transducer (Fig. 3.10). This plot demonstrates that only a small portion of the transducer face was generating any pressure.

It was hypothesised that a manufacturing fault had caused the transducer to only transmit ultrasound from such a small area at the centre of its face. Since the transducer housing is opaque, the placement of components was

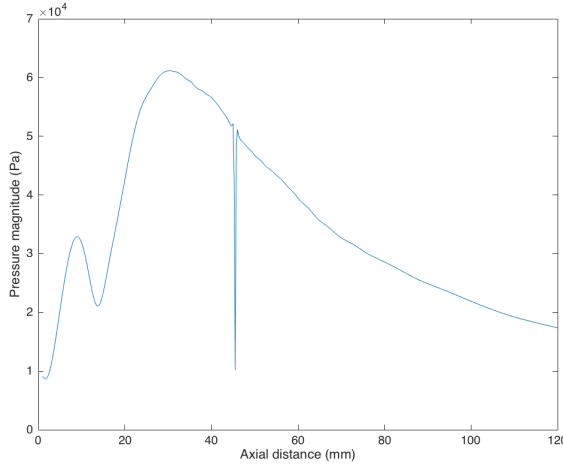
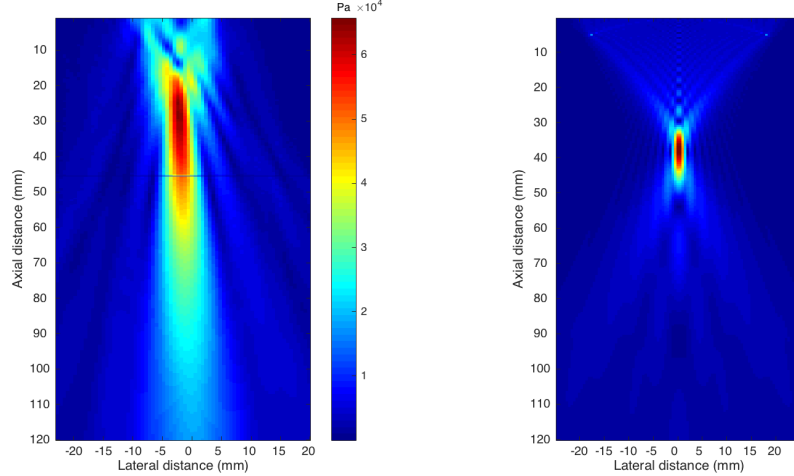


Figure 3.8: The magnitude of the pressure along the beam axis of the acoustic field generated by Transducer 1. The sharp trough at 45 mm from the transducer is an artefact from the projection algorithm.



(a) XZ-plane from the acoustic field generated by Transducer 1. The line across the plane at 45 mm from the transducer is an artefact from the projection algorithm.

(b) XZ-plane from the acoustic field simulated for an ideal bowl transducer with the same geometry as Transducer 1.

Figure 3.9: Comparison of XZ-planes from the acoustic fields (a) generated by Transducer 1 and (b) simulated for an ideal transducer of the same geometry.

3.2 Development of Design (Transducer 2)

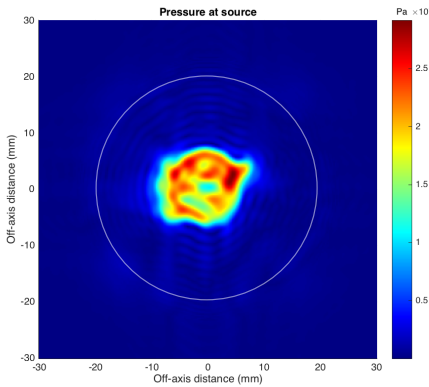


Figure 3.10: The acoustic pressure on the surface of Transducer 1. The white circle shows the size of the transducer.

assessed using x-ray photographs of the transducer (Fig. 3.11).³ These images reveal that the QWML does not cover the whole face of the PZT disc: there is an air gap around the outside. This gap inhibits the transmission of ultrasound, meaning that pressure is only generated at the centre of the transducer’s face. The x-ray images also demonstrate that the thermocouple junction remained correctly placed and is fixed in the correct position inside the housing, embedded in the urethane foam.

Figure 3.11 shows that there is too little epoxy-tungsten mixture inside the transducer. This could have been caused by leakage through the hole at the thinnest part of the lens (Section 3.1.2) or because too little was inserted in the first place. The design of the housing for Transducer 1 allows little tolerance for the wrong amount of QWML material to be inserted: if too much is placed on the face of the PZT disc then the QWML will be too thick. This was addressed as part of the development of the housing design.

3.2 Development of Design (Transducer 2)

Transducer 1 demonstrated that a functioning ultrasound transducer can be built using RP techniques. However, changes were necessary in several aspects of the design. A second transducer was designed to implement these changes (Section 3.2.1).

³These photographs were taken by Marco Endrizzi in the UCL Dept Medical Physics & Biomedical Engineering.



Figure 3.11: X-ray images of Transducer 1. These images show the air gap between the PZT disc and the back of the lens (red ellipses).

In addition to the developments described in Section 3.2.1, the housing for Transducer 2 was printed with VeroClear (Stratasys, RGD810) material.⁴ This material is more expensive than VeroBlackPlus, however it allowed the placement of components to be evaluated after manufacture without needing to take x-ray images. VeroClear has very similar acoustic properties to VeroBlackPlus, so no changes were made to the design to account for this change in manufacturing method.

3.2.1 Modifications and Improvements to Design

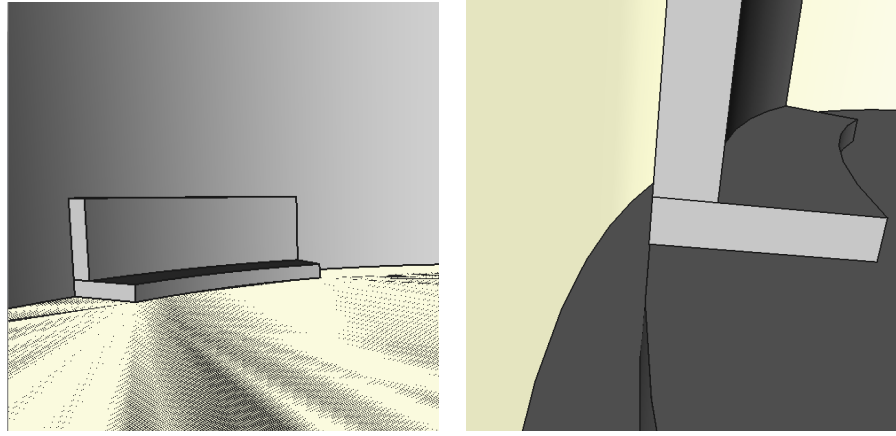
The changes to the design for the second major iteration were made in two areas: the fixings for the PZT disc and the formation of the QWML, and the lens.

PZT Mount and QWML

In order to allow an excess of QWML material to be inserted into the housing during manufacture—to ensure that the whole face of the PZT disc was covered—the ridge that ran around the outside of the bottom of the housing cavity was broken into three segments (Fig. 3.12). These segments also contain vertical guides to ensure the PZT disc is positioned correctly inside the housing. The gaps between each segment allow any unnecessary epoxy-tungsten mixture to move outwards, allowing for an excess to be used during

⁴This material was not available in the Dept Medical Physics & Biomedical Engineering, so the print was processed by the Bartlett Manufacturing and Design Exchange at the Bartlett School of Architecture.

3.2 Development of Design (Transducer 2)



(a) Pedestal and vertical guide for the placement of a PZT disc inside the housing. The base of the pedestal is the thickness of the QWML; the vertical guide ensures the disc is centred with the housing.
(b) The trough around the inside edge of the housing. The trough collects the excess QWML material.

Figure 3.12: Sections of the CAD model of the housing for Transducer 2.

the manufacture. This ensures that plenty of QWML was used to ensure a good connection between the PZT disc and the bottom of the housing.

A trough runs around the inside edge of the transducer housing (Fig. 3.12b). This collects any excess QWML and prevents it from rising up and making an electrical connection between the top and bottom electrodes of the PZT disc.

These adaptations made the transducer housing wider than in previous designs: it has an outer diameter of 47 mm.

Lens mount

Objective 3 (Section 1.3) requires detachable lenses to be built and tested. In order to use Transducer 2 with these lenses, it was given a plane face. A 2 mm ridge was added to the front of the transducer—around the sonicating surface—which would be used to attach the lenses (see Chapter 5)

Manufacture

Transducer 2 was assembled following the same process as Transducer 1 (Section 3.1.2). Since the PZT disc used for Transducer 2 was identical to



Figure 3.13: Transducer 2.

that used in Transducer 1, its impedance was not measured and an identical matching network was built.

The transparent housing allowed the spread of the QWML to be verified once it had been built (Fig. 3.13).

3.2.2 Acoustic Characterisation

The acoustic characterisation of Transducer 2 was performed using the same experimental setup as the equivalent measurements for Transducer 1 (Section 3.1.3).

The last axial maximum of a circular plane piston transducer is located at a distance of

$$z_{\text{LAM}} = \frac{a^2}{\lambda} \quad (3.1)$$

from the transducer face, where a is the radius of the transducer, and λ is the wavelength.^[20] Therefore the expected location of the last axial maximum of Transducer 2 was 243 mm. The pressure along the beam axis has a complex near-field region (as expected) and the last axial maximum is approximately 190 mm from the transducer (Fig. 3.14).

An XZ-plane was calculated using the Rayleigh integral and compared to a simulation of an ideal plane piston transducer of the same size and at

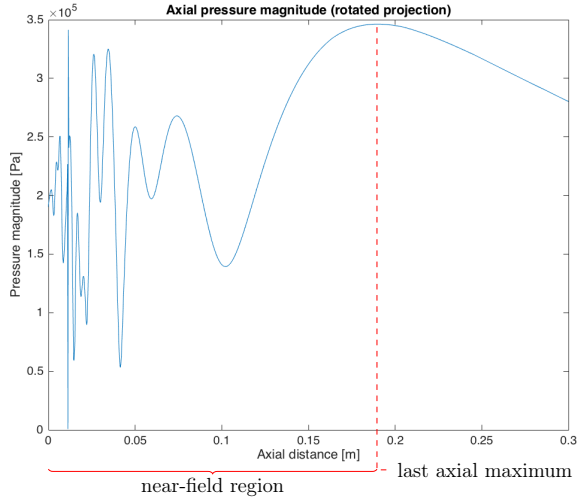
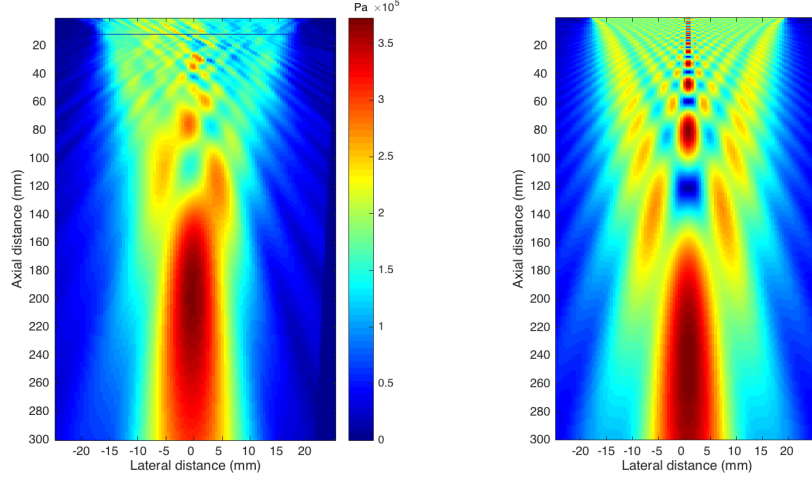


Figure 3.14: The magnitude of the pressure along the beam axis of the acoustic field generated by Transducer 2. The complex near-field region and the last axial maximum are labelled.

the same frequency (Fig. 3.15).⁵ This comparison shows good qualitative agreement between the measured output of Transducer 2 and the expected output of an ideal transducer.

To further verify that the entirety of the face of the transducer was generating acoustic pressure, the Rayleigh integral was used to calculate the pressure at the surface of the transducer (Fig. 3.16). This demonstrates that there was pressure generated across the whole face of Transducer 2, however it was not uniform. To investigate this asymmetry, a medical ultrasound imaging system (BK Ultrasound, SonixMDP) was used to probe the structure of the transducer. Transducer 2 was placed in a small tank of water; the front of the imaging probe (BK Ultrasound, L14-5/38 GPS Linear) was submerged in the tank and the beam was moved across the face of Transducer 2. The transducer was inspected to identify any faults which may have caused the asymmetric acoustic response (Fig. 3.17). The structure behind the transducer face appeared to be uniform in these images, therefore no cause could be identified from this experiment.

⁵The transducer was not well aligned with the motorised axes during this scan. However, the projection of the measured field was rotated in three dimensions in MATLAB to produce Figs. 3.14 and 3.15a.



(a) XZ-plane from the acoustic field generated by Transducer 2. The line across the plane at 11 mm from the transducer is an artefact from the projection algorithm.

(b) XZ-plane from the acoustic field simulated for an ideal plane piston transducer with the same geometry as Transducer 2.

Figure 3.15: Comparison of XZ-planes from the acoustic fields (a) generated by Transducer 2 and (b) simulated for an ideal transducer of the same geometry.

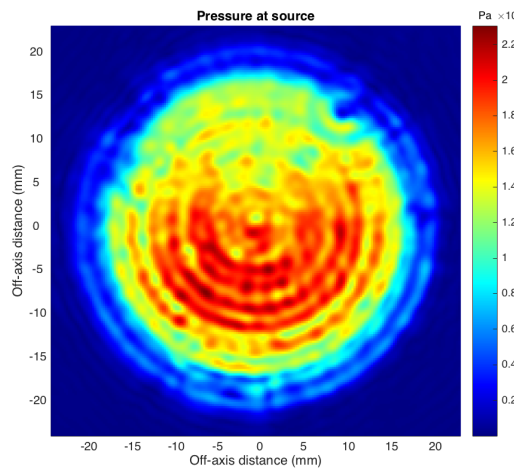


Figure 3.16: The acoustic pressure on the surface of Transducer 2.

3.2 Development of Design (Transducer 2)



Figure 3.17: Ultrasound image of the front of Transducer 2. The ridge for attaching lenses is in the top left corner. The two strong lines are the face of the transducer and, below that, the front face of the QWML.

3.2.3 Temperature Response

The peak pressure generated by Transducer 2 in previous experiments was 350 kPa (Section 3.2.2). In order to generate the pressures required for High Intensity Focused Ultrasound (HIFU) (see Section 1.1) the transducer would need to be driven with more power. As more power is transmitted to the transducer, it will heat up. In order to understand this heating, measurements were made using a thermocouple embedded in the transducer housing (see Section 3.1.1).

Transducer 2 was placed in a small tank of deionised water, facing an acoustic absorber to prevent reflections from the side of the tank. The transducer was connected to a signal generator (Agilent, 33522A) through a 53 dB RF amplifier (Electronics & Innovation, 1020L); a high-impedance scope probe (Agilent, N2863B) was used to measure the voltage at the input of the transducer with an oscilloscope (Agilent, DSO-X 3024A) (Fig. 3.18). The thermocouple was plugged into a temperature logger (National Instruments, 01A2083D). The signal generator amplitude was adjusted to drive the transducer at 40–80 V peak-to-peak. The temperature was recorded every second as the transducer was driven by a continuous signal for three minutes then allowed to cool for one and a half minutes. One of these measurements was curtailed because the temperature reached 45 °C; above this temperature VeroClear may begin to deform.^[21] The temperature change over time at

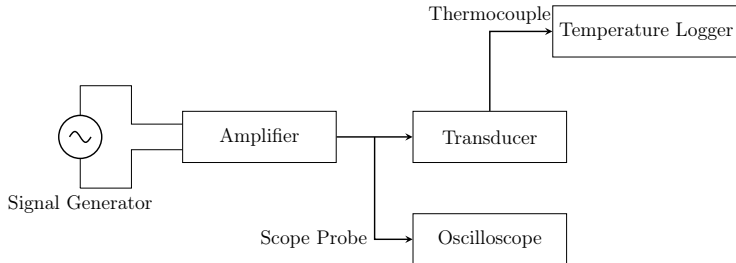


Figure 3.18: Diagram of the setup used to investigate the thermal response of Transducer 2.

each of these driving voltages shows a classical heating profile (Fig. 3.19a).

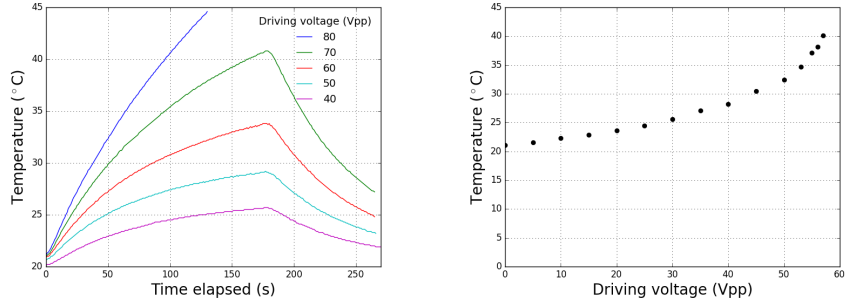
It was observed that as the transducer heated, the measurement of the amplitude of the driving signal (at the transducer input) increased. It is hypothesised that this is caused by the change in the efficiency of the power transfer to the transducer caused by its changing electrical impedance as it heats.

In order to determine the maximum steady-state input voltage (*i.e.* the input voltage when the temperature and voltage at the transducer input have reached an equilibrium) at which Transducer 2 can safely be driven, the above setup was used to drive the transducer until such an equilibrium was reached at input voltages of 0–60 V peak-to-peak, and the maximum temperature was recorded (Fig. 3.19b). These measurements demonstrate that Transducer 2 can be safely driven up to 57 V peak-to-peak, however above this level the temperature quickly exceeds the safe limit. To investigate the acoustic pressure generated by driving Transducer 2 at 50 V, the measurements conducted with the transducer driven by a 10 V peak-to-peak signal (Section 3.2.2) were scaled linearly. The pressure at the face of the transducer (Fig. 3.16) was multiplied by five and projected forward using the Rayleigh integral to find a peak pressure of approximately 1.8 MPa. This is an unfocused field; it is therefore hypothesised that the focusing gain for a focused field from Transducer 2 could produce pressures suitable for HIFU applications.

3.3 Conclusions

Several iterations of a design for a RP single-element ultrasound transducer were designed, including two which were built. A workflow was developed

3.3 Conclusions



- (a) The thermal response of Transducer 2. The transducer was driven in continuous wave mode for 3 minutes and allowed to cool for 1.5 minutes.
- (b) The equilibrium temperature of Transducer 2 at different driving voltages.

Figure 3.19: Results of experiments to characterise the thermal response of Transducer 2.

to build large single-element transducers and suitable construction materials were identified and sourced.

Each iteration of the design built on the previous, with improvements made to improve the quality of the transducer. The acoustic responses of these transducers were successfully characterised: the second (Transducer 2) generates an acoustic field which is comparable to an ideal transducer of the same geometry. This transducer can generate acoustic fields with a pressure amplitude of up to 1.8 MPa without risk of damage to the transducer due to heating. This will allow pressures suitable for HIFU to be created when sufficient focusing is performed.

Cost Analysis

Each of these transducers cost very little to manufacture. The 3D printing for Transducer 1 cost £12.72.⁶ Transducer 2 was printed on the more expensive VeroClear material, which cost £20. The cap for each transducer cost £4.32.

The other components for the manufacture of these transducers were bought in bulk, so it is difficult to specify the cost for each element. The only significant expense was the tungsten powder, 1 kg of which cost £80, however each transducer required only approximately 5 g. Thus the contribution of

⁶A £5 admin fee applied to each use of the printer. This charge was applied many times during the development of the project, however the print bed is large enough that many transducers could be printed at once, making this cost negligible.

these components, bought in comparatively large quantities, is very small. However, the electronic components cost £5.47 for each transducer. This means the cost per transducer was approximately £30.

Chapter 4

Smaller Transducer Elements

In order to construct arrays of ultrasound transducers, elements smaller than the 38 mm transducers described in Chapter 3 need to be designed. These were built with smaller lead zirconate titanate (PZT) discs with a diameter of 10 mm.

4.1 Design

Two variations of small elements were designed: both had a flat plane face—without a ridge for attaching a lens—and were 4 cm long. This length allowed the transducers to be easily held by a clamp for testing; it is possible that future versions of the small elements could be shorter, but the additional length makes them easier to handle. Because there was very little space inside the housing of these transducers—and to avoid making the transducers larger than necessary—the electrical impedance matching network was built externally on stripboard (Vero Technologies, 09-1034). A cap for the rear of the transducer, incorporating a hole for the BNC socket, was designed to be similar to the caps for Transducers 1 and 2.

The lower part of the housings for Transducers 4.1 and 4.2 had two pins on the outside. This was to allow them to slot into a BNC-like socket in a frame; this feature was left out of future designs because there have been no frames for multi-element arrays designed for this project. The difference between the two transducers was the method by which the PZT disc was attached in the housing and connected to the driving circuit.

The first variation (Transducer 3.1) used a scaled-down version of the

4.2 Design Development

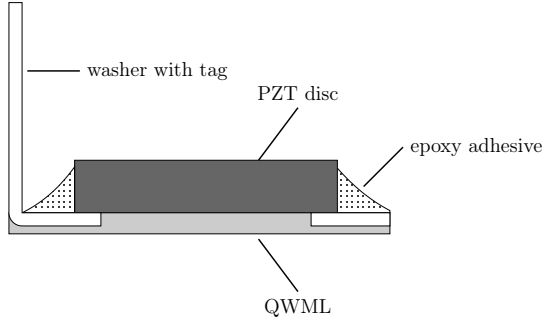


Figure 4.1: Cross-section a PZT disc mounted on a metal washer. A metal tag extends vertically from the washer, allowing an electrical connection to the front (lower) face of the electrode to be easily soldered. The PZT disc is held in place by a small amount of epoxy adhesive.

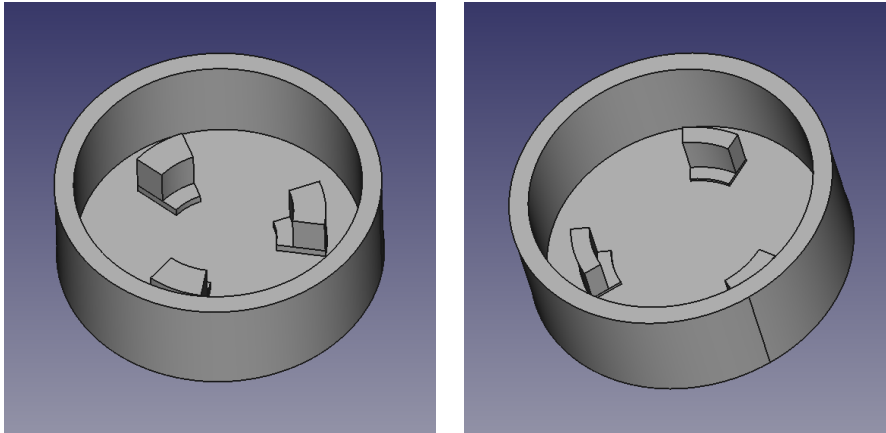
mount used in Transducer 2: the PZT disc sat directly on three standoffs, held in place by tall guides. Since the face of the PZT disc was too small for a solder joint, wires were attached to the front and rear faces with a conductive silver epoxy adhesive (MG Chemicals, 8331) (Fig. 4.3c).

The second variation (Transducer 3.2) utilised a washer with a tag (taken from a BNC socket): the PZT disc sat on the washer, which had an internal diameter of 9 mm. The disc was held in place by an epoxy adhesive and this assembly sat on top of the QWML (Fig. 4.1). The washer acted as an extension to the front electrode; a wire was soldered to the metal tag extending from the washer to create an electrical connection, and the conductive epoxy was used to connect the wire on the rear electrode (Fig. 4.3c). The washer sat on three segments inside the transducer housing.

When these transducers were built, it was found to be extremely difficult to insert the components into the narrow housing. Two attempts were made to assemble Transducers 3.1 and 3.2, however each time the components were poorly aligned inside the housing or the connections to the electrodes were broken.

4.2 Design Development

In order to overcome the difficulty of manufacturing transducers with such small piezoelectric elements, the housing was deconstructed into a further two sections. The main body of the transducer became a hollow tube; the front section, on which the PZT discs were mounted, became a second cap



(a) Model of the cap with a mounting structure for a PZT disc only.

(b) Model of the cap with a structure for the PZT disc mounted on a metal washer.

Figure 4.2: Computer Aided Design (CAD) models of the caps designed to contain the quarter-wave matching layer (QWML) and PZT discs used in Transducers 4.1 and 4.2.

that attached to the housing tube in a similar way to the cap at the rear. On the inside of this cap was the mounting segments for the PZT disc (Fig. 4.2). This design allowed easier access to the PZT mounting section, allowing the components to be held in place as the epoxy adhesive mixtures cured.

Two designs were made, corresponding to the mounting structures from Transducers 3.1 and 3.2.

4.3 Manufacture

Transducers 4.1 and 4.2 took significantly longer than Transducers 1 and 2 (Chapter 3) to build. Each step of the manufacture required an epoxy adhesive, and each application of the adhesive was left to cure for several (8–24) hours. Consequently, the manufacture of these smaller elements took several days. The silver epoxy required the components to be held in place for five hours as it cured; this was achieved by using Blu Tack (Bostik) (see Figs. 4.3a and 4.3d).

The first step in the manufacture of both small transducers was to solder wires to the washers and BNC sockets. Wires longer than the length of the final transducers were used to allow easy access to the ends while the three

4.3 Manufacture

components of the housing were separated. Transducer 4.1 and 4.2 then had different build processes due to the different mounting mechanisms. The second step in the assembly of Transducer 4.1 was to use the conductive epoxy to attach wire to the front electrode (Fig. 4.3d). The front electrode of the disc was then covered with the epoxy-tungsten mixture (the QWML; see Section 2.2) and placed on the support segments in the first cap. Once this mixture had cured, the second wire was threaded through the rear cap and the housing tube before being attached to the rear electrode.

Transducer 4.2 was assembled similarly: the washer and PZT disc were placed together and held in place with Blu Tack. The epoxy-tungsten mix was spread on the face of the pair and they were placed in the mounting cap, held in place with Blu Tack (Fig. 4.3a). When the QWML had cured, the Blu Tack was removed and the second wire was threaded through the rear cap and the housing tube before being attached to the rear electrode.

The three components of each of the transducer housings were then put together and the joins were sealed with epoxy adhesive (Araldite, ARA-400001). Coaxial cables were attached to the transducers and the join was wrapped in self-amalgamating tape (RS Pro, 494-449) (Fig. 4.4).

The impedance of these transducers was measured using an impedance analyzer (Wayne Kerr, 6500B) fitted with a component fixture (Wayne Kerr, 1011).¹ The impedance of Transducer 4.1 immersed in water, at 1 MHz, was measured to be $(5.9996 - 5.9771i)\Omega$. The impedance of Transducer 4.2 was similarly measured to be $(41.2793 - 529.58i)\Omega$. These were matched to the source impedance (50Ω) with step-up networks (see Section 2.3 and Fig. 2.2a). The values of the components in the step-up network were calculated using a MATLAB script (see Section 2.3) to be 8.6nF and $3.5\mu\text{H}$ for Transducer 4.1 and 1.5nF and $87.3\mu\text{H}$ for Transducer 4.2. The matching network for Transducer 4.1 was built with a 4.7nF , a 2.2nF , and a 1.8nF capacitor in parallel—equivalent to a single 8.7nF capacitor—and a $3.3\mu\text{H}$ inductor (Bourns, RLB1314-3R3ML). The matching network for Transducer 4.2 was built with a 1.8nF capacitor and a $90\mu\text{H}$ inductor (Roxburgh EMC, SMV80). These were both built on stripboard; the capacitors were provided by Dr Xiao Liu from stock kept in the Department of Electronic & Electrical Engineering (Fig. 4.5).

¹This measurement was conducted with help from Dr Xiao Liu of the Dept Electronic & Electrical Engineering.

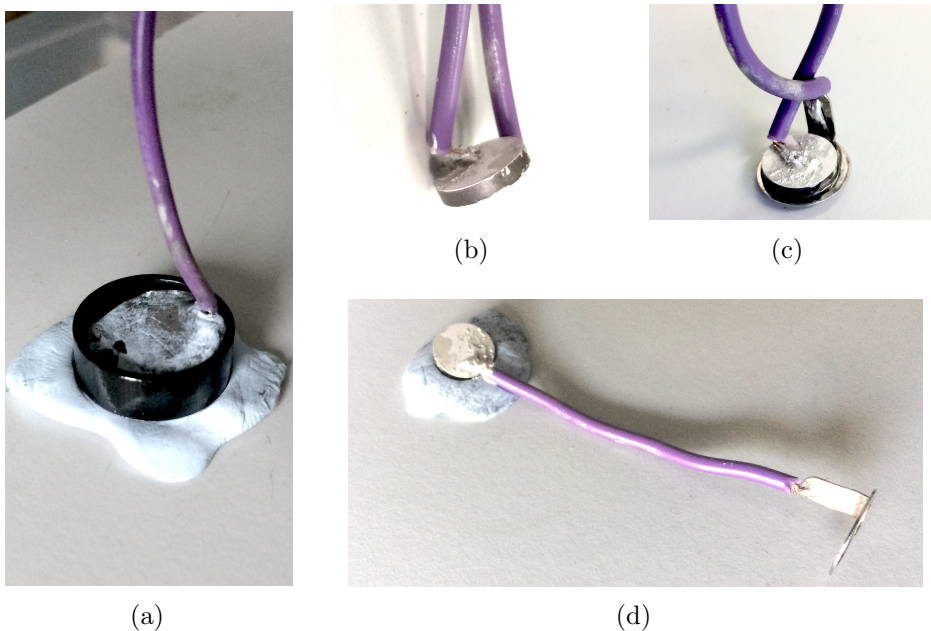


Figure 4.3: Stages of the assembly process for Transducers 4.1 and 4.2. Blu Tack is used to hold the components in place as the epoxy adhesives used to connect the wires to the PZT discs and in the QWML cure.



Figure 4.4: Transducers 4.1 and 4.2.

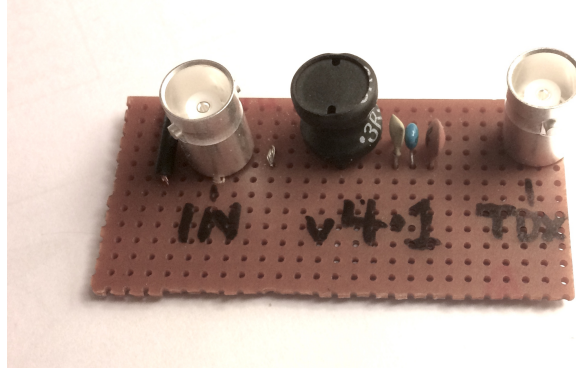


Figure 4.5: The electrical impedance matching network for Transducer 4.1. This is a step-up network built on stripboard.

4.4 Conclusions

The large transducer designs have been scaled down to build smaller single element-transducers with 10 mm-wide PZT discs. The characteristic response of these transducers have not been measured due to time constraints. However, a workflow for the assembly of these transducers has been designed to manage the complexity of working with small parts.

The housing parts for both Transducers 4.1 and 4.2 cost only £11.56 to be 3D printed. The other components for the manufacture of these transducers were bought in bulk when the larger transducers were built, so it is difficult to specify the cost for each element. Since these components were bought in large quantities, the cost per transducer is very small. The capacitors were provided by Dr Xiao Liu (see Section 4.3). However, the other electronic components cost £12.65. This means the cost per transducer was approximately £12.

The PZT discs used for these transducers were provided free as samples, however they would cost approximately £14 each if bought in quantities of less than 100.² Therefore the cost of building these small elements in the future would be approximately £26.

²€16.30 per unit. This was approximately £14.05 when this report was written.

Chapter 5

Detachable Lenses

Lenses can be used to generate specific acoustic fields (see Section 2.5). Detachable lenses allow many different fields to be generated by the same transducer. Fabricating these lenses with Rapid Prototyping (RP) techniques allows many different acoustic fields to be generated quickly and cheaply. The designs in this section are fast and cheap to build; in the case of the acoustic kinoform, the entire design process is automated, and it would be simple to automate all lens design work.

For this project, two types of detachable lens were designed to be attached to Transducer 2: a focusing lens and an acoustic kinoform.

5.1 Focusing Lens

5.1.1 Design

The focusing lens was designed to have a focal length twice the width of the transducer (*i.e.* an $f/2$ lens): 76 mm. Since the speed of sound in VeroBlackPlus is known (2495 m s^{-1}),^[17] Eq. (2.9) can be used to calculate the desired radius of curvature to be 46.9 mm.

A Computer Aided Design (CAD) model of the $f/2$ focusing lens was created with a back that would fit with the ridge and plane face of Transducer 2 (see Section 3.2.1). This lens was printed in VeroBlack, as show in Fig. 5.1.

5.1.2 Acoustic Characterisation

The acoustic field generated through the focusing lens was measured in an acoustic scanning tank following the same procedure as for Transducers 1



Figure 5.1: The focusing lens built for Transducer 2. The lens has a focal length of 76 mm. These images show the (a) front at (b) back of the lens.

and 2 (Section 3.1.3). The pressure was recorded at all points on a 80×80 point plane—with a point spacing of 0.5 mm—34.6 mm from the face of the transducer.

The peak pressure along the beam axis has a peak at the expected distance from the transducer face (Fig. 5.2). The acoustic pressure on an XZ-plane was calculated using the Rayleigh integral from the recorded pressure values and this was compared with a simulated plane from an ideal transducer with the same geometry as the lens (Fig. 5.3).¹ The comparison shows a good qualitative agreement between the measured and simulated data. However, the focal region of the 3D printed lens is larger and the focus is further away from the transducer than expected. This might be because VeroBlackPlus is very absorbing (see Section 3.1.1), so the thicker edge of the lens (as opposed to the thin central region) will cause apodization, reducing the focusing power of the lens.

To investigate the possible apodization, the Rayleigh integral was used to calculate the pressure on the face of the focusing lens (Fig. 5.4). This demonstrated that the pressure at the edge of the lens was much lower than in the central region, confirming the apodising effect of the high absorption of VeroBlack. The asymmetry of the field at the surface of the lens can be

¹The transducer was not well aligned with the motorised axes during this scan. However, the projection of the measured field was rotated in three dimensions in MATLAB to produce Figs. 5.2 and 5.3a.

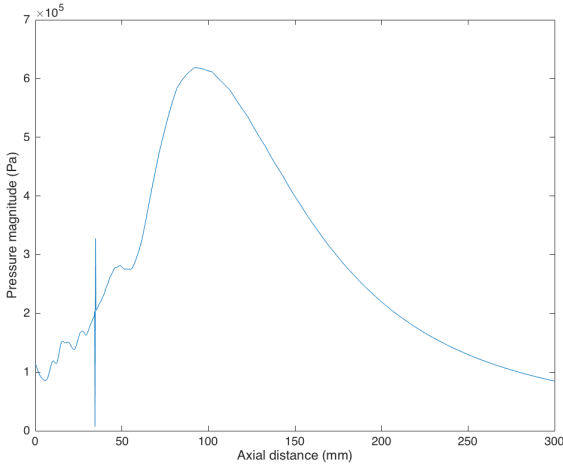
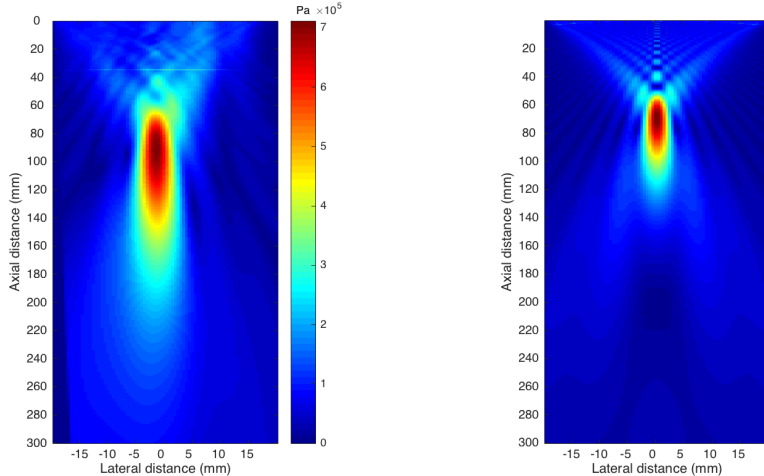


Figure 5.2: The magnitude of the pressure along the beam axis of the acoustic field generated by Transducer 2 with the focusing lens attached. The sharp trough at 35 mm from the transducer is an artefact from the projection algorithm.



(a) XZ-plane from the acoustic field generated by Transducer 2 with the focusing lens attached. The line across the plane at 35 mm from the transducer is an artefact from the projection algorithm.

(b) XZ-plane from the acoustic field simulated for an ideal bowl transducer with the same geometry as Transducer 2 with the lens attached.

Figure 5.3: Comparison of XZ-planes from the acoustic fields (a) generated by Transducer 2 with the focusing lens attached and (b) simulated for an ideal transducer of the same geometry.

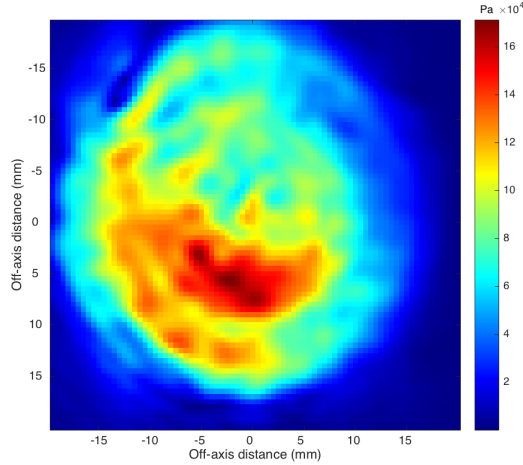


Figure 5.4: The acoustic pressure on the surface of the focusing lens driven by Transducer 2.

attributed to the asymmetry in the field generated by Transducer 2 in the absence of a lens; Fig. 3.16 in Section 3.2.2 shows that the acoustic field on the surface of Transducer 2 has the same asymmetry demonstrated in Fig. 5.4.

5.2 Acoustic Kinoform

A kinoform (see Section 2.5) was designed and attached to Transducer 2 using MATLAB code provided by Michael Brown.^[22] This script was modified to use the material properties and dimensions relevant for Transducer 2, including adding a backing to the kinoform to allow it to attach to the front of the transducer by fitting into the ridge designed for that purpose (see Section 3.2.1). The script takes an input image and produces a map of the thickness of the kinoform in the desired size, to generate that image in a pressure field at a given distance. The script also creates a 3D object file that can be sent to a printer.

A kinoform was fabricated to generate the image of a cross at a distance of 30 mm from the transducer. This simple image was chosen to demonstrate that a kinoform could be successfully designed and printed for Transducer 2. The acoustic field generated through the focusing lens was measured in an acoustic scanning tank following the same procedure as for Transducers 1



Figure 5.5: The acoustic kinoform.

and 2 (Section 3.1.3). The pressure was recorded at all points on a 50×50 point plane—with a point spacing of 0.25 mm—33.3 mm from the face of the transducer, using a hydrophone with a 0.2 mm piezoelectric element (Precision Acoustics, 2402). The pressure at a distance of 30 mm from the transducer was calculated from the measured plane using the Rayleigh integral (Fig. 5.6). The reconstruction of this image from the measurements of the acoustic field generated with the kinoform demonstrates that an effective acoustic hologram can be built quickly and at low cost.

5.3 Conclusions

Both a focusing lens and an acoustic kinoform have been designed, printed and tested. Both lenses produce acoustic fields that closely match the desired fields.

A workflow has been established for creating kinoforms from arbitrary input images, using a script that builds the 3D object file directly.

The focusing lens cost £2.76 to print and the kinoform cost £2.18.

5.3 Conclusions

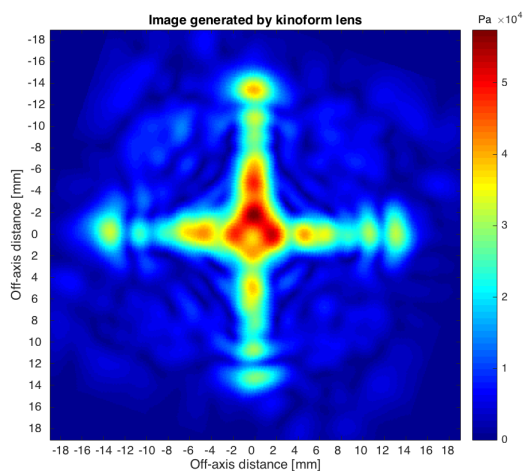


Figure 5.6: The pressure generated by Transducer 2 with the acoustic kinoform attached at a distance of 30 mm from the transducer face.

Chapter 6

Summary & Conclusions

6.1 Summary

The aim of this project was to demonstrate that ultrasound transducers can be built quickly and at low cost using Rapid Prototyping (RP) techniques. This would be achieved by designing several ultrasound transducers in an iterative design process and characterising their acoustic and thermal responses. The project also aimed to demonstrate the use of 3D printed lenses to produce custom acoustic fields using these transducers.

Several iterations of a large single element-transducer have been designed (Chapter 3). Modifications have been made to each successive design in order to improve it: the later designs generated acoustic fields that were more representative of the ideal transducers they were designed to emulate. A workflow for building these transducers has been established and two have been built using RP techniques.

Transducer 2 has been shown to generate an acoustic field close to that of an ideal transducer (Section 3.2). Its thermal response has been characterised and a safe upper limit for driving voltage has been established. This driving power allows the transducer to generate a field with a pressure amplitude of 1.8 MPa, which is hypothesised to be sufficient for High Intensity Focused Ultrasound (HIFU) applications.

Smaller elements suitable for use in ultrasound arrays have been designed and built (Chapter 4). The designs have been developed to make the assembly of the elements simpler and more robust. These elements have not been characterised acoustically, but their construction has informed design

6.2 Future Development

improvements and demonstrated that small elements are possible using RP techniques.

It has been demonstrated that detachable lenses can be produced quickly and at low cost using RP techniques (Chapter 5). These lenses can produce focused acoustic fields or, in the case of kinoforms, specific pressure patterns. A workflow has been established that allows kinoform objects to be generated from a given image programmatically.

The large single-element transducers cost approximately £30 each. The small transducers cost approximately £12 each (although future transducers would require the purchase of additional lead zirconate titanate (PZT) discs, so would cost approximately £26). The focusing lens and the acoustic kinoform cost approximately £2.50 each. These prices are significantly less than the costs incurred per transducer by Kim *et al.*^[3] (see Section 1.1). Thus this project demonstrates that RP techniques can be used within the Biomedical Ultrasound Group (BUG) to produce single-element ultrasound transducers at a dramatically lower cost than commercially available transducers.

6.2 Future Development

In order to allow BUG to use the techniques developed in this project to build ultrasound arrays quickly and at low cost, the small elements would have to be placed in a frame. This would require the design of a frame for a particular application, and development of the mechanism to fix the elements in place within it.

The work on kinoforms could be expanded upon by building a kinoform for a more complicated image and by testing the limits of the resolution that can be achieved using Transducer 2.

In order to make the design and production of single-element transducers easier and faster, a full workflow for programmatically generating printable objects from the necessary parameters could be established. It has been demonstrated that MATLAB can produce functioning kinoforms given the correct information and this could be expanded to allow transducer arrays to be produced quickly to generate given acoustic fields.

Appendix A

List of Designed Parts

A.1 Transducers

This is a list of the transducers which have been built.

Name	Parts used	Notes
Transducer 1 (tdxv1)	<code>housing_mk-1-2</code> <code>cap_mk-1-1</code>	VeroBlackPlus; matching layer only in centre of lens; $f/1$ (38 mm); k-type thermocouple
Transducer 2 (tdxv2)	<code>housing_mk-2-2</code> <code>cap_mk-1-2-1</code>	VeroClear housing, VeroBlack-Plus cap; no focus; k-type thermocouple
Transducer 4.1 (tdxv4.1)	<code>housing_mk-4_housing-tube</code> <code>housing_mk-4-1_pzt-mount</code> <code>cap_mk-1-3-1</code>	VeroBlackPlus; external matching network
Transducer 4.2 (tdxv4.2)	<code>housing_mk-4_housing-tube</code> <code>housing_mk-4-2_pzt-mount</code> <code>cap_mk-1-3-1</code>	VeroBlackPlus; external matching network

A.2 Designed Parts

This is a list of the parts designed to be 3D printed. Some of these are iterations that were never manufactured.

A.2.1 Transducer Housings

Filename	Notes	Date
housing_mk-1-1	Internal diameter too small	2016-10-17
housing_mk-1-2		2016-10-23
housing_mk-2-1	redundant	2016-12-05
housing_mk-2-2	flat lens	2016-12-08
housing_mk-2-3	curved lens ($f/2$)	2016-12-08
housing_mk-3-0	for OD10 PZT	2017-02-01
housing_mk-3-1	with shelf for PZT and pins	2017-02-03
housing_mk-3-2	as above, but different mounting	2017-02-22
housing_mk-4_housing-tube	Hollow tube	2017-03-02
housing_mk-4-1_pzt-mount	cap for above	2017-03-02
housing_mk-4-2_pzt-mount	cap for above	2017-03-02

A.2.2 Transducer Caps

Filename	Notes	Date
cap_mk-1-1	Incl. hole for thermocouple	2016-11-13
cap_mk-1-2	redundant	2016-12-05
cap_mk-1-2-1	Incl. hole for thermocouple	2016-12-08
cap_mk-1-3-1	For small element	2017-02-14

A.2.3 Lenses & Attachments

Filename	Notes	Date
<code>lens_f-2_mk-1</code>	$f/2$ (76 mm); for tdxv2	2017-01-21
<code>kinoform</code>	cross hologram for tdxv2	2017-02-23

References

- [1] G. ter Haar, “Acoustic Surgery,” *Physics Today*, 54, no., pp. 29–34, 2001, ISSN: 0031-9228. DOI: [10.1063/1.1445545](https://doi.org/10.1063/1.1445545).
- [2] H. A. S. Kamimura, S. Wang, H. Chen, Q. Wang, C. Aurup, C. Acosta, A. A. O. Carneiro, and E. E. Konofagou, “Focused ultrasound neuro-modulation of cortical and subcortical brain structures using 1.9 MHz,” *Medical Physics*, 43, no., pp. 5730–5735, 2016, ISSN: 00942405. DOI: [10.1118/1.4963208](https://doi.org/10.1118/1.4963208).
- [3] Y. Kim, A. D. Maxwell, T. L. Hall, Z. Xu, K.-w. Lin, and C. A. Cain, “Rapid Prototyping Fabrication of Focused Ultrasound Transducers,” *IEEE Transactions on Ultrasonics, Ferroelectrics, and Frequency Control*, 61, no., p. 22, 2014. DOI: [10.1016/B978-1-4557-2818-3.00009-1](https://doi.org/10.1016/B978-1-4557-2818-3.00009-1).
- [4] M Sano, S Yousefi, and L Xing, “WE-EF-210-07: Development of a Minimally Invasive Photo Acoustic Imaging System for Early Prostate Cancer Detection,” *Medical Physics*, 42, no., pp. 3684–3684, 2015, ISSN: 00942405. DOI: [10.1118/1.4926030](https://doi.org/10.1118/1.4926030).
- [5] M. Cheverton, P. Singh, L. S. Smith, K. P. Chan, J. A. Brewer, and V. Venkataramani, “Ceramic-Polymer Additive Manufacturing System for Ultrasound Transducers,” in *Annual International Solid Freeform Fabrication Symposium*, Austin, Texas, USA, 2012.
- [6] H. Chabok, C. Zhou, Y. Chen, A. Eskandarinazhad, Q. Zhou, and K. Shung, “Ultrasound Transducer Array Fabrication Based on Additive Manufacturing of Piezocomposites,” in *ASME/ISCIE 2012 International Symposium on Flexible Automation*, St. Louis, Missouri, USA, 2012, pp. 433–444. DOI: [10.1115/ISFA2012-7119](https://doi.org/10.1115/ISFA2012-7119).

REFERENCES

- [7] Z. Chen, X. Song, L. Lei, X. Chen, C. Fei, C. T. Chiu, X. Qian, T. Ma, Y. Yang, K. Shung, Y. Chen, and Q. Zhou, “3D printing of piezoelectric element for energy focusing and ultrasonic sensing,” *Nano Energy*, 27, no., pp. 78–86, 2016, ISSN: 22112855. DOI: 10.1016/j.nanoen.2016.06.048.
- [8] G. Gautschi, *Piezoelectric Sensorics*. Berlin, Heidelberg: Springer Berlin Heidelberg, 2002, ISBN: 978-3-642-07600-8. DOI: 10.1007/978-3-662-04732-3. [Online]. Available: <http://link.springer.com/10.1007/978-3-662-04732-3>.
- [9] “Pz26 (Navy I) datasheet,” Ferroperm Piezoceramics, Kvistgaard, Tech. Rep. [Online]. Available: <http://www.ferroperm-piezo.com/files/files/Pz26Datasheet.pdf>.
- [10] B. Cox and B. Treeby, *MPHY3900: Ultrasound in Medicine lecture notes*, London, 2016.
- [11] *Ferroperm Pz26*. [Online]. Available: <http://piezomat.org/materials/286> (visited on 10/08/2016).
- [12] R. A. Webster, “Passive materials for high frequency piezocomposite ultrasonic transducers,” PhD thesis, The University of Birmingham, 2009. [Online]. Available: <http://etheses.bham.ac.uk/1311/>.
- [13] A. Maxwell, (*Senior Fellow, University of Washington*), Personal communication, 2016.
- [14] *Polycraft 010 - Soft Foam*. [Online]. Available: <http://www.mbfq.co.uk/foam-materials/foam-soft.html> (visited on 10/24/2016).
- [15] K. Melde, A. G. Mark, T. Qiu, and P. Fischer, “Holograms for acoustics,” *Nature*, 537, no., pp. 518–522, 2016, ISSN: 0028-0836. DOI: 10.1038/nature19755.
- [16] V. A. Shutilov, *Fundamental Physics of Ultrasound*. Glasgow: CRC Press, 1988, ISBN: 9782881246845.
- [17] D. Nikitichev, E. Alles, S. Noimark, W. Xia, and A. Desjardins, “Acoustic properties of 3D printed materials and their application,” 2016.
- [18] *FreeCAD*. [Online]. Available: <http://www.freecadweb.org/> (visited on 10/03/2016).
- [19] E. Martin, (*Research Associate, UCL*), Personal communication, 2016.

- [20] F. A. Duck, A. C. Baker, and H. C. Starritt, Eds., *Ultrasound in Medicine*, ser. Series in Medical Physics and Biomedical Engineering. CRC Press, 1998, ISBN: 9781420050370. [Online]. Available: <https://books.google.co.uk/books?id=JtCmJysD8JoC>.
- [21] *Rigid Translucent/Clear / RGD810 (VeroClear)*. [Online]. Available: <https://www.xometry.com/materials-rigid-translucentclear-rgd810-veroclear/> (visited on 01/23/2017).
- [22] M. Brown, (*PhD Student, UCL*), Personal communication, 2017.